

The effect of continuous furnace load organization on temperature distribution during controlled atmosphere brazing process

Slawomir NADOLNY^{1,2} , Michał ROGALEWICZ¹ , and Adam HAMROL¹ 

¹ Poznan University of Technology, Faculty of Mechanical Engineering, Poland

² MAHLE Behr Ostrów Wielkopolski Sp. z o.o., Poland

Abstract. Aluminum heat exchangers (AHEXs) represent a continuously evolving production sector with applications across various industries. Their mass production utilizes continuous furnaces combined with the controlled atmosphere brazing (CAB) process. The required heat is supplied through convection, conduction, and radiation. The degree of these interactions and their impact on the temperature achieved inside an AHEX can vary significantly depending on the type and mass of the load. The additional tooling, such as brazing jigs, also plays a crucial role. The design of these jigs, including their material and mass, is essential for the heat delivered inside an AHEX. The presence of brazing jigs can enhance conduction and radiation effects but may also reduce convection. Due to the use of different heating elements, varying lengths of continuous furnace chambers, and a nitrogen atmosphere control system, it is necessary to tailor the heating profile (furnace parameters) individually for each type of AHEX. The heating and cooling rates, as well as the duration in the elevated temperature, including the maximum temperature achieved inside an AHEX, are critical. This article presents a study on the impact of continuous furnace load organization (including load density and the presence of brazing jigs) on the temperatures achieved inside an AHEX.

Keywords: CAB; aluminum heat exchangers; brazing jig; heat capacity; heat conductivity.

1. INTRODUCTION

1.1. Aluminum heat exchangers

Aluminum heat exchangers (AHEXs) are used for the exchange of thermal energy between different solid bodies, between solids and fluids, or between fluids. They are utilized in devices, machinery, and buildings in processes where temperature regulation is required, such as heat recovery in refining processes, glass production, cement production, and metallurgy [1, 2]. Increasingly, they also form a crucial part of HVAC (heating, ventilation, and air conditioning) systems in commercial and residential buildings, especially with the gradual rise of intelligent building design since the 1970s [3]. Thanks to their lightweight properties, AHEXs are used in all types of vehicles, including rail, marine, and aviation transportation.

However, the largest share of AHEXs can be observed in the automotive industry. Currently, the use of cooling modules for air conditioning systems (i.e., condenser, evaporator, and heater) or drive and control systems (i.e., oil cooling) is standard. Additionally, they are also applied in charge of air cooling, exhaust gas cooling, and fuel cooling [4]. Considering the scale of automotive production, which reached 94 million units in the year 2023, and the use of various types of AHEX in each vehicle, this represents a vast scale of applications [5].

The design of an AHEX is developed according to specific requirements for heat flow, resilience, and energy losses, depending on the intended application. For this reason, there are various types of AHEXs, which can be grouped, for example, based on design, efficiency, compactness, coolant phases, or heat transfer mechanisms [2].

AHEXs are constructed from components subjected to various technological processes, mainly stamping, and rolling. They are structured as multilouver centers arranged alternately with multiport tubes enclosed by reinforcement plates and headers, an example of which is shown in Fig. 1.

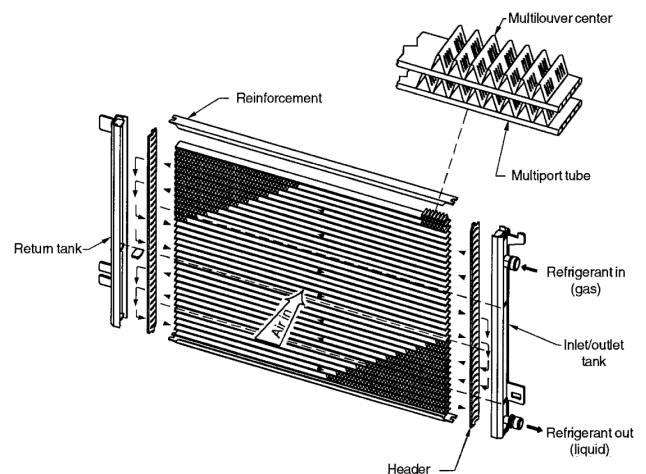


Fig. 1. Scheme of micro-channel aluminum heat exchanger [6]

*e-mail: slawomir.nadolny@doctorate.put.poznan.pl

Manuscript submitted 2024-09-09, revised 2024-09-09, initially accepted for publication 2025-02-11, published in May 2025.

1.2. Brazeability

Due to the constant circulation of the coolant, a tight connection between the components is required. This is achieved using brazing technology, where all contact areas between components require the formation of a brazed joint.

Achieving the so-called “brazed construction properties”, which ensures that the AHEx meets the specified requirements, is a complex concept defined by the term “brazeability”. This term includes the structural features of the AHEx, the materials used, brazing conditions, and operational properties. Various criteria are used to assess brazeability, including joint preparation, dimensions, assembly gap size, type of additional materials (brazing alloy, flux, atmosphere), and heating conditions, including the brazing technology used [7].

The formation of the brazed joint results from the diffusion of silicon due to the Kirkendall effect, which is significantly influenced by temperature and the fit between the components [8]. It is recommended that the peak temperature achieved inside the AHEx falls within the melting range of the filler metal alloy but does not approach the melting temperature of the base aluminum material. In practice, this means an optimal brazing temperature range of 590–610°C [9]. Failure to reach this temperature will prevent the brazing process from occurring. On the other hand, exceeding it can result in localized hot spots, leading to fouling precursors that initiate chemical reactions with organic compounds. This, in turn, promotes surface corrosion by hindering the formation of a protective aluminum oxide layer [6]. The heating rate, including the uniformity of temperature distribution, is also significant. Slow heating could result in a more even temperature distribution inside the AHEx, but it also facilitates undesirable magnesium diffusion processes and may dry out the flux, making brazing more difficult [10]. For this reason, a rapid temperature increase, up to 45°C/min, is recommended. However, such a rapid rise complicates the maintenance of uniform temperature distribution inside the AHEx. Additionally, the recommended duration for the AHEx to remain within the brazing temperature range is 3–5 minutes, with local temperature differences not exceeding ±5°C [11]. This is due to the negative interaction of erosion/dissolution during the contact of the molten filler metal with the base aluminum material, which intensifies with time [8].

1.3. Heat transfer

Heat can be distributed inside the AHExs through various heat transfer methods. Depending on the environment and transfer conditions, convection, conduction, and radiation are distinguished, which often occur simultaneously, to varying degrees.

Convection is the transfer of heat by the movement of a fluid, which can be a liquid or a gas. It results from the macroscopic movement of molecules along with their thermal energy. When the fluid is heated, it becomes less dense and rises, while cooler, denser fluid sinks, creating a circulation that transfers heat. Convection can be natural, driven by density differences due to temperature variations, or forced, induced by external forces (e.g., a pump or fan) [12].

Conduction is the process of heat transfer through direct molecular contact. Heat moves from a region of higher tem-

perature to a region of lower temperature within the same body or between touching bodies. Beyond the wall boundary layer, conduction has a much smaller impact on heat transfer compared to convection [12].

Radiation is the transfer of energy via electromagnetic waves, such as infrared radiation. It does not require direct contact or a medium for heat transfer, meaning it can occur even in a vacuum. Radiation depends on the emissivity coefficient ϵ , which is dimensionless and ranges from 0 to 1, with 1 representing an ideal black body that is a perfect emitter and absorber of radiation [12].

1.4. Continuous furnace

In the mass production of AHExs, controlled atmosphere brazing (CAB) is the most often used technology [4]. This process takes place in continuous furnaces, resulting in low unit costs and flexibility in the brazing process [13]. Heating of the load (i.e., AHExs) is achieved through a combination of different heating elements. These include gas-fired burners (unshielded flames) or resistance heaters (radiant tube burners, electric heaters, jet cooling). For burners, convection is the dominant heat transfer method, whereas for resistance heaters, it is radiation [14]. Radiation is the preferred method for heating products of similar dimensions in continuous mode. However, for more complex products, it may be necessary to provide more varied brazing conditions with an emphasis on increased convection through so-called convection preheating. This solution enhances the flexibility of the CAB process, allowing simultaneous brazing of AHExs with different masses and shapes [2].

To control the effects of radiation and convection, continuous furnaces are divided into successive chambers [14]. Furnaces can vary in total length and therefore the number and size of chambers, the arrangement of heating elements, or additional functions, such as a recuperator, afterburner, or dry scrubber. The nitrogen supply (atmosphere control) system and the oil vapor removal system are also significant and can vary. An example of a continuous furnace division is shown on Fig. 2.

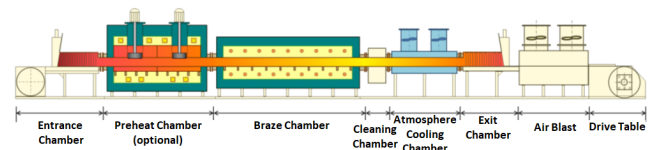


Fig. 2. Division of the continuous furnace (convection-radiation furnace) into chambers [15]

1.5. Temperature measurement

Due to the inclusion of chambers in the design of the continuous furnace, in addition to the settings of the furnace (heating profile) for each chamber, it is also necessary to control the temperatures achieved by the AHEx itself during the CAB process, including its maximum temperature, the rate of temperature rise, and the time spent in elevated temperature. For this purpose, the Datapaq® measurement method is used. It involves precise temperature recording over time using thermocouples connected to the interior of the AHEx. Since the measurement apparatus

The effect of continuous furnace load organization on temperature distribution during controlled atmosphere brazing process

must be present inside the continuous furnace along with the load, a special protective barrier in the form of a thermal shield is used [16]. The results are presented in the form of a time-temperature cycle, which example of is illustrated in Fig. 3.

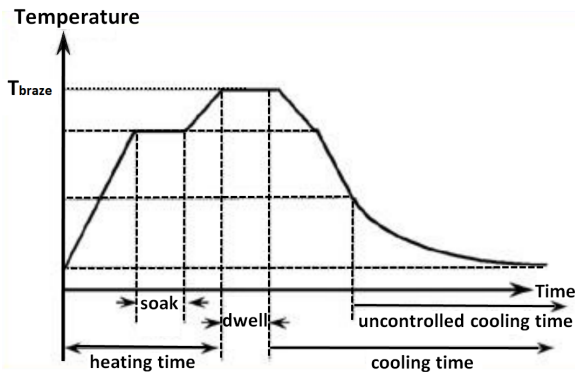


Fig. 3. Time-temperature cycle in continuous furnace for the CAB proces [11]

1.6. Materials and tooling

The successful execution of the CAB process, in addition to the AHEX design, is also influenced by the composition of the materials used (alloys), including surface morphology and additional tooling [9, 17, 18].

The selection of alloys for individual components is based on specific requirements depending on the intended use including their operating conditions and performance requirements. For example, in the case of automotive AHEXs, they are subjected to vibrations and frequent changes in pressure and temperature. Therefore, alloys containing magnesium additives (e.g., AW 3003) are used [10]. The presence of Mg improves the strength of the AHEX but simultaneously negatively affects brazability for instance due to the phenomenon known as magnesium needling [17].

Additional tooling, known as a brazing jig (an example of which is shown in Fig. 4), in the form of a housing in which the AHEX is mounted, is mainly used to maintain the connections between components via compression during the continuous furnace process. In addition to differences in their shape and mass, brazing jigs may vary in the materials used for construction or the principle of operation [18]. Adjusting their design and thermal parameters is crucial not only for ensuring the formation of brazed joints in the desired areas of the AHEX but also for achieving the expected temperature and atmosphere within the individual chambers of the continuous furnace.

Brazing jigs are typically made from a special corrosion-resistant steel alloy (e.g., 316L) or graphite. The brazing jigs, along with the AHEXs, form the load in the continuous furnace. Depending on their shape and material, and therefore their mass, they are subject to varying degrees of convection and radiation. Additionally, being in direct contact with the AHEXs, they also transfer heat through conduction. The average temperature of the load is inversely proportional to its mass within the individual chambers of the continuous furnace [19]. Therefore, the number of brazing jigs along with the AHEXs, and thus their joint

density within the furnace chamber, can significantly impact the values obtained in the time-temperature cycle.

2. RESEARCH PROBLEM

The research presented in this article is part of ongoing studies aimed at reducing the amount of flux residue after the CAB process for AHEXs used in the automotive industry [17]. The objective was to determine the influence of load organization in the continuous furnace, including its density, and the presence of brazing jigs, on the achieved time-temperature cycle.

In the time-temperature cycle, the temperature inside the AHEX during the CAB process is measured over time. However, temperature itself is merely the result of heat, which is the kinetic and potential energy of micro-particles delivered to the material. Heat is regulated by the first law of thermodynamics, which states the conservation of energy. Heat transfer occurs spontaneously from one body to another in the direction of decreasing temperature, under the second law of thermodynamics. The heat exchange is dependent on the temperature gradient, proportional to the heat flux, as dictated by Fourier's law of heat conduction [12, 20]. As a result, the material reaches a measurable elevated temperature, which is necessary to initiate atomic diffusion [21], enabling the formation of the brazed joint.

The movement of atoms is referred to as thermal motion, driven by thermal energy. The higher the temperature, the more extensive this motion becomes. In the case of solids, thermal motion is limited to vibrations. However, in liquids (gases and fluids), when the material is in equilibrium, atoms can move in any direction with equal probability, effectively neutralizing atomic transport. When this equilibrium is disturbed (e.g., due to a difference in material composition), atomic movement is no longer entirely random. This results in a shift in a specific direction, leading to the equalization of concentration differences. This movement is known as atomic diffusion. Concentration changes occur particularly at high temperatures. It is important to note that materials consist of different phases – regions of material where atoms are arranged in a specific manner. This is known as the phase crystalline structure and influences the thermal motion and, in effect, the atomic diffusion [22].

The degree of heat change relative to the temperature of a material is defined by its heat capacity, which indicates the amount of thermal energy required to raise the temperature of a given mass of the material by one degree Kelvin. The degree of heat transfer through the material is defined by its thermal conductivity. This property affects the functionality of the material at elevated temperatures by determining its efficiency in transporting heat through direct contact between molecules. Thermal conductivity is influenced by convection, conduction, and radiation, as heat is primarily conducted by electrons and phonons [23]. A low thermal conductivity value is desirable when minimizing heat loss is the goal, whereas an increase in this parameter indicates enhanced heat transport from one location to another.

The examined AHEX units are composed of various components, primarily made of aluminum AW3003, which is one of the most widely used alloys in the CAB process. They are man-

ufactured through rolling and stamping methods, with a total weight of approximately 1.5 kg. The composition of this alloy is presented in Table 1.

Table 1

Content of alloying elements of aluminum AW-3003 [25]

Element		Mn	Fe	Si	Cu	Zn	Al	Other
Wt [%]	Min	1	0	0	0.05	0	96.8	Residual
	Max	1	0	0	0.05	0	96.8	

On the other hand, the used brazing jigs are made of stainless steel 316L with reduced carbon content and weigh approximately 3.5 kg. This material is an austenitic steel known for its exceptional corrosion resistance. The low carbon content minimizes carbide precipitation, which can cause intergranular corrosion during operation at elevated temperatures [24], such as in a continuous furnace. The composition of stainless steel 316L is shown in Table 2.

Table 2

Content of alloying elements of stainless steel 316L [26]

Element		Cr	Ni	Mo	Mn	Fe	C/Si/N/S/P
Wt [%]	Min	16	10	2	0	63	Residual
	Max	18	14	3	2	72	

AHEXs have a complex construction, consisting of connections between components made of different alloys and additional materials such as filler metal, flux, and machining oils. Therefore, the resultant heat capacity and thermal conductivity values, especially their changes at elevated temperatures, do not directly result from the dominant material used in their construction and would require further analysis. The AHEXs are mounted in brazing jigs of specific shape and mass, for which thermal properties have also not been measured. Additionally, the CAB process occurs in a variable atmosphere and temperature, and consequently under varying pressures, which are controlled only at specific points through the set parameters (heating profile). This means that the values necessary to create a heat flow model inside the continuous furnace are not known [27].

Despite the unknown thermal properties of the AHEXs and jigs, they are consistent. Similarly, the heating profile is constant for a given type of AHEX. However, the parameter that can be controlled under these conditions is the organization of the load in the continuous furnace. In the examined CAB process, a conveyor belt is used, on which the AHEX units mounted in brazing jigs are placed. They are arranged sequentially in rows of three for the entire production batch. Changing the density of the AHEXs arrangement or not mounting them in brazing jigs results in a decrease in the mass and properties of the load inside the continuous furnace chamber. In such cases, a significant effect on the temperature achieved by the AHEXs over time is expected.

3. METHODOLOGY

For the given study, 54 AHEX units were prepared and then divided into three groups of 18 units each. Each group was further divided into three production batches of six units each. For each batch, 2 Datapaq® measurements were taken on the first AHEX and another two on the last one. As a result, 12 time-temperature cycle graphs were obtained for each AHEX group. The identified groups were divided as follows:

- a) Control group – AHEXs subjected to the standard process used for this type of product. This involves the use of brazing jigs and the density of distribution determined by the size of the continuous furnace conveyor belt. As a result, 12 AHEX units were present simultaneously in the longest chamber of the continuous furnace, corresponding to a load weight of approximately 60 kg. The arrangement of the AHEXs mounted in brazing jigs in the control group, along with a description of the furnace chamber elements, is shown in Fig. 4.

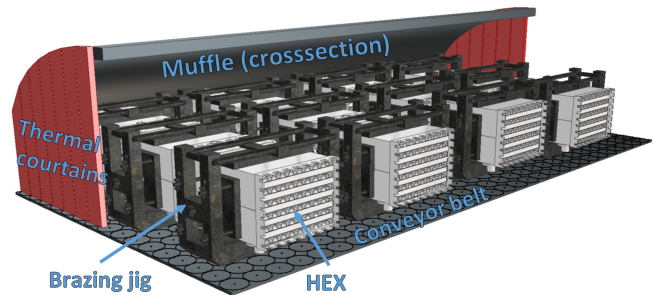


Fig. 4. Scheme of arrangement of heat exchangers in the furnace for the control group along with a description of the continuous furnace chamber elements [Author's own]

- b) AHEXs brazed with spacing (single) – These AHEX units were mounted in standard brazing jigs, but their distribution density on the conveyor belt was adjusted so that only a single AHEX was present in the longest furnace chamber at a time, resulting in a load weight of approximately 5 kg. Figure 5 shows the arrangement of such AHEX.

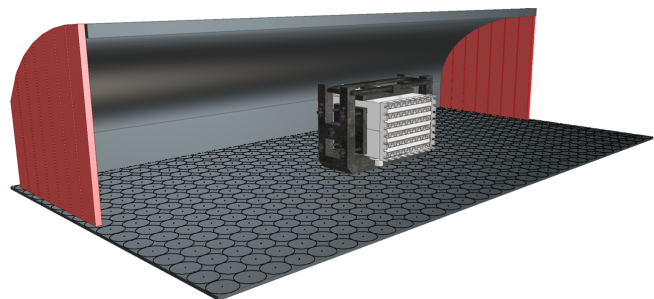


Fig. 5. Scheme of arrangement of heat exchangers in the furnace for the single group [Author's own]

- c) AHEXs brazed without jigs (bare) – These are AHEX units loaded into the furnace without the brazing jigs. To allow safe transport during the process, they were placed in a special basket made of stainless steel 316L, weighing approx-

imately 15 kg and storing six AHEx units. This resulted in approximately 50 kg of load in the longest chamber at a time. The arrangement of these AHEx units is shown in Fig. 6.

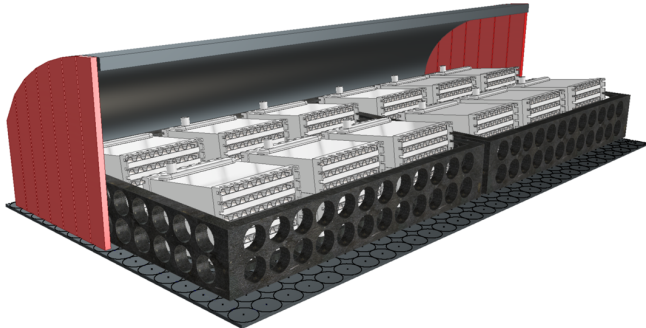


Fig. 6. Scheme of arrangement of heat exchangers in the furnace for the bare group [Author's own]

The temperature was measured using Datapaq® equipment with thermocouple sensors, the construction of which is shown in Fig. 7. The thermocouple consists of two wires made of dissimilar metals joined together at one end, forming the measurement area T_{TC} . At the other end, the wires serve as the signal conditioning circuit path. By using the so-called Seebeck voltage V_{TC} and comparing it to the reference temperature area T_{CJ} , it is possible to determine the temperature of the tested object [28]. The thermocouples were connected to a data logger, which collected temperature data inside the AHEx and assigned it to the time duration of the measurement. In each tested AHEx, the thermocouples were inserted to a consistent depth near its outer edges. The data obtained was recorded as a time-temperature cycle graph. The measurements from both thermocouples in a single AHEx were averaged. The following areas of the brazing process were identified:

- a) Degreasing phase – The temperature rise inside the AHExs from ambient temperature to a local maximum in the range of 250–350°C. This temperature results from the use of self-evaporating oil required in stamping and rolling processes. Failure to perform this phase may prevent the formation of the brazed joint, which requires, among other things, a clean surface [29]. The duration of this phase is the same for all groups, as it depends on the fixed speed settings of the con-

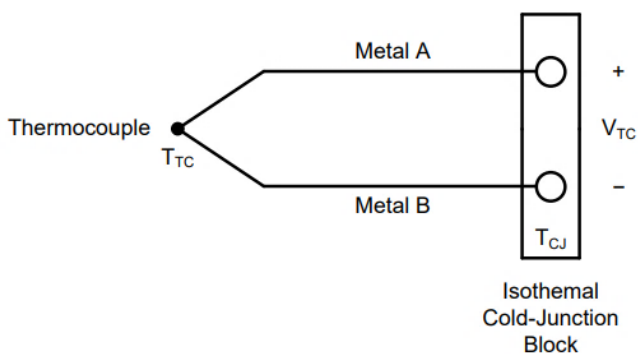


Fig. 7. Scheme of the thermocouple [28]

tinuous furnace conveyor belt and the length of the chambers. The evaporation chamber includes an exhaust system that prevents oil vapors from escaping into the atmosphere outside the furnace.

- b) Breath phase (“Soak time”) – This phase additionally allows gases to evacuate from inside the AHExs. It takes place during the transition between the furnace chambers from degreasing to heating. Due to the absence of heating elements, this phase appears as a temperature drop on the time-temperature cycle graph with a fixed duration, also due to the constant conveyor speed.
- c) Heat-up phase – The temperature rises until it reaches 577°C, which is the approximate melting point of the used flux.
- d) 577°C+ phase – The area from when the AHExs reach the temperature of 577°C until it falls back to that value. This occurs in a nitrogen atmosphere, where oxygen levels are below 100 ppm.
- e) 590°C+ phase – The area from when the AHExs reach a temperature of 590°C until it falls back to that value. This range marks the start of the “brazing window”, which signifies the conditions required for forming the brazed joint: no oxygen, melted flux, and melted filler metal.
- f) Cool-down phase – The area where the temperature of the AHExs drops from 577°C to 250°C. The selected lower value is established due to a lack of precise knowledge of when the AHExs exit the last chamber of the continuous furnace and begin uncontrolled cooling.

To compare the individual phases, the coordinates of their start and end points were determined. For the defined phases, the area under the time-temperature cycle graph was calculated in the given temperature range $[\Delta T]$, multiplied by the duration of the phase [min]. The resulting unit used is the time-temperature cycle phase area (TTC_{PA}) [°C·min].

However, it is important to note that the temperature increase inside the AHExs is not linear, especially at lower temperatures, and the equation of the function represented by the graph is not known. For this reason, the established analysis method involves a TTC_{PA} value error, which is most significant for the degreasing phase, presumably underestimating the actual value by approximately 30%. However, this error is consistent across all measurements, hence it was concluded that it does not affect the drawn conclusions. For the other phases, the greatest discrepancy was noted in the heating phase, where the error presumably underestimates the real TTC_{PA} value by approximately 2%.

4. RESULTS

The significant temperatures obtained in the AHEx groups are presented in Table 3, while Table 4 shows the start and end times for each of the phases. The data from the tables is represented in Fig. 8, which provides a graphical representation of the time-temperature Cycle graph, considering the division of groups. Additionally, using the control group as an example, the breakdown of individual phases is shown, for which the TTC_{PA} values were determined, including the maximum temperature of the degreasing phase, the minimum value of the Breath phase,

S. Nadolny, M. Rogalewicz, and A. Hamrol

Table 3

Significant temperature milestones recorded for the measured AHExs groups

Group	Control	Single	Bare
Degreasing phase Max temperature [°C]	336	350	352
Breath phase Min temperature [°C]	316	313	311
Max temperature reached [°C]	602	606	593

Table 4

Time range of the selected phases for the measured AHExs groups

Phase	Control		Single		Bare	
	Start [min]	End [min]	Start [min]	End [min]	Start [min]	End [min]
Degreasing	0	15.5	0	15.5	0	15.5
Breath	15.5	20.3	15.5	20.3	15.5	20.3
Heat-up	20.3	38.5	20.3	38.6	20.3	42.2
577°C+	38.5	50.3	38.6	52.5	42.2	51.7
590°C+	43.7	50.3	43.4	51.3	48.2	50.1
Max temperature	46.8		48.4		49.1	
Cool-down (250°C)	50.3	67.1	52.5	67.7	51.7	66.8

and the maximum achieved temperature. The cool-down phase was measured only until the temperature drops to 250°C, as the graph does not clearly indicate the onset of uncontrolled cooling, which begins after the AHExs exit the last chamber of the continuous furnace.

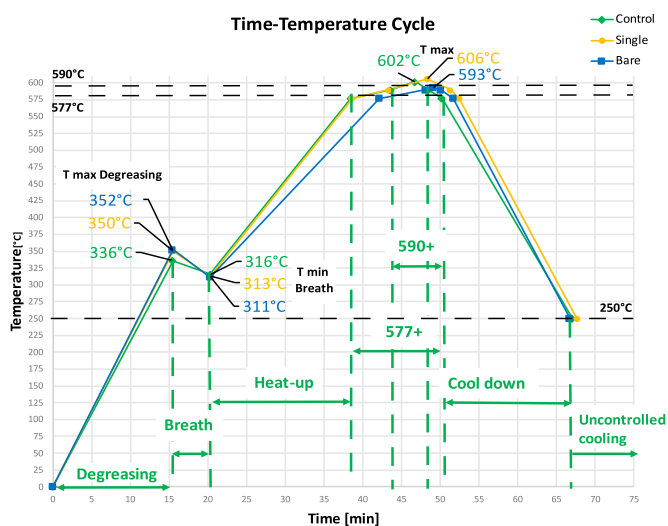
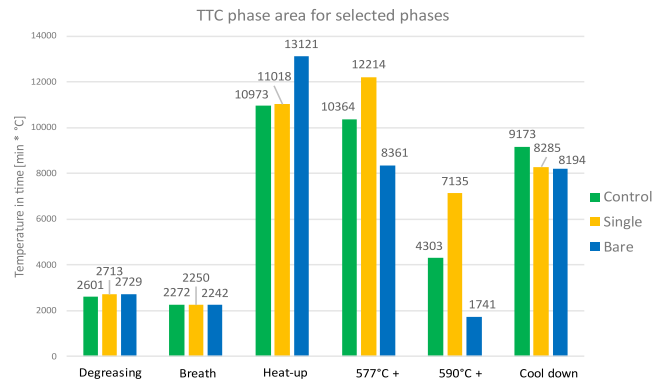
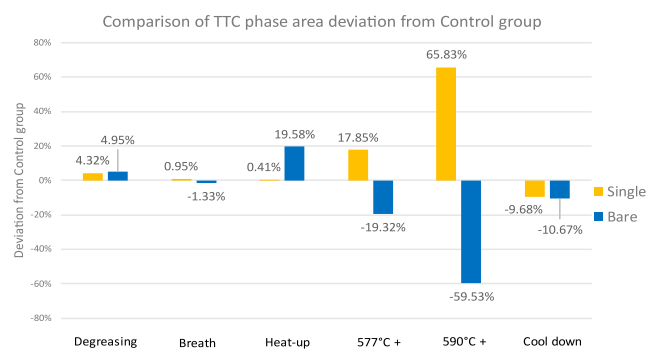
**Fig. 8.** Time-temperature cycle for control, single and bare AHExs groups divided into CAB phases with their peak temperatures

Figure 9 presents the calculated TTC_{PA} values for the different groups, divided by phase, while Fig. 10 shows the spread of the single and bare groups compared to the control group for each phase. The following conclusions were drawn:

**Fig. 9.** TTC_{PA} values for individual phases divided by the groups**Fig. 10.** Comparison of the TTC_{PA} value spread for the single and bare groups to the control group

- Degreasing phase – the highest TTC_{PA} value was obtained in the bare group. However, the low range value (5 percentage points) indicates that differences in radiation and convection effects in this phase are negligible, regardless of the load mass and arrangement. This could be due to the exhaust system removing the evaporated oil.
- Breath phase – the highest TTC_{PA} value was recorded for the single group, but the low range value (2 percentage points) suggests that the impact of load arrangement and mass on this phase is negligible. It can also be noted that the role of brazing jigs as the heat sink, due to the short duration of this phase, also has no significant impact.
- Heat-up phase – similar results were observed between the single and control groups, indicating that the influence of load mass in this phase is negligible. Only in the bare group, there is a noticeable increase in TTC_{PA} values (20 percentage points). It can thus be inferred that the type of load plays a crucial role in this phase. The brazing jigs, working as heat sinks, retrieve heat from the AHExs. Hence, their lack in the bare group boosts the effectiveness of convection in reaching the elevated temperatures inside the AHExs.
- 577°C+ phase – clear differences are evident between all AHEx groups. A high range value (37 percentage points) indicates that both the type and mass of the load are significant. The highest TTC_{PA} value in the single group highlights the importance of load mass, and thus the influence of heat flow on forced convection. Additionally, the lowest TTC_{PA}

value in the bare group suggests that the influence of radiation is rising together with the temperature levels. The brazing jigs, heated up in the previous phase, continue to absorb heat through radiation. In effect, they allow for heat transfer to the AHExs through conduction, increasing the recorded temperature.

- e) 590°C+ phase – the influences from the previous phase are more distinct, where both the type and mass of the load remain important. However, it is worth noting that the difference between the groups is much larger (126 percentage points). The maximum temperature reached in the groups significantly affects this phase duration. The lowest temperature recorded in the bare group causes this phase to last 3 times shorter than in the control group. Where the highest temperature reached in the single group increases the duration by 20%. It can be inferred that radiation allows it to reach higher temperatures. The presence of the brazing jigs enhances its effectiveness and enables additional heat transfer through conduction.
- f) Cool-down phase – the results show the highest TTC_{PA} value for the control group. This indicates that both the type and mass of the load have a significant impact in this phase, but the low range value (11 percentage points) suggests that this impact is limited. This could be a result of heated air evacuation outside the chamber, preventing significant retention of convective heat released by the AHExs inside of it.

5. CONCLUSIONS

The results obtained indicate that optimizing the CAB process requires consideration of the material and mass of the brazing jigs. Mismatched parameters can lead to significantly higher energy consumption to achieve the same temperature inside the AHExs, generating additional process costs. An important note is that the presence of brazing jigs is crucial for reaching elevated temperatures, where radiation begins to play a more significant role than convection.

The collected data suggest that when designing brazing jigs, attention can be paid to areas of the AHEx where higher local temperatures are required due to the greater overall thickness of the assembled components or different thermal parameters of the used alloys. In these areas, compression can be achieved using materials with lower heat capacity, compared to the AHEx material, such as stainless steel 316L. However, for thin-walled areas where elevated temperatures could pose a risk of overheating, brazing jig materials with higher heat capacity, such as graphite, could be preferred.

The experiment allowed for achieving both increased and decreased maximum temperatures inside the AHExs without the need to change the heating profile.

The significance of this comes from the change-over process, where the production must be halted, and the conveyor belt emptied before the heating profile can be changed. Afterwards, a stabilization period for the changed temperature is also required. The experiment confirms the possibility of reducing these costs and increasing process efficiency through the organization of the load within the continuous furnace alone.

However, the study did not consider different materials for brazing jigs. The obtained results highlight the potential for further research on matching the design and material of brazing jigs to ensure uniform temperature distribution in desired areas of the AHEx. Such efforts could ultimately lead to energy savings by requiring shorter brazing cycles at lower temperatures inside chambers. At the same time, it could reduce defects caused by thermal mismatches inside the AHEx, which, in large-scale production, could translate into significant cost savings in scrap material.

6. DISCUSSION

Both the components of AHExs and the brazing jigs are made from a combination of different materials produced through various manufacturing processes. As a result, they may differ in microstructure, and consequently, in thermal properties [24]. For aluminum, this variation is due to changes in the morphology of the Al-Si eutectic, which can be lamellar, acicular, or fibrous, depending on the production technology [30]. The influence of alloying element concentrations on thermal conductivity is also well-documented. For example, a 1% addition of certain elements decreases thermal conductivity from 6% down to 54% for Si [30].

The effect of these elemental additions on density, heat capacity, and thermal conductivity is presented in Table 5, comparing the alloys used to pure base materials (aluminum and iron) and to graphite, which can also be used to manufacture brazing jigs [18].

Table 5

Thermal properties of selected materials at temperature 20°C [24, 26, 31–37]

Material	Density [kg/m ³]	Specific heat capacity [J/g·K]	Heat conductivity [W/m·K]
Aluminium	2700	897	237
Aluminium AW3003	2730	890	140–160
Iron	7200	449	94
Stainless steel 316L	7900	500	15
Graphite	1750	710	160

In the case of the AW3003 alloy compared to pure aluminum, the influence of alloying elements can be observed as a slight increase in density and heat capacity (~ 1%), but a significant decrease in thermal conductivity (~ 60%). On the other hand, for stainless steel 316L, compared to pure iron, the influence of alloying elements results in a noticeable increase in density and heat capacity (~ 10%) and a significant decrease in thermal conductivity (~ 78%).

The use of graphite in brazing jigs instead of stainless steel 316L would result in a decrease in density (load mass) by ~ 73%, and an increase in heat capacity, causing slower heating) by ~ 42%, and an increase in thermal conductivity, significantly

affecting the heating rate and possibly the maximum temperature of the AHEx, by $\sim 1,000\%$.

Significant differences in heat capacity and thermal conductivity arise from the increased activity of atoms acting as heat carriers, as well as changes in the crystalline structure of the material, which alter the level of scattering [38].

The temperature inside the furnace is determined by the combined effects of used heating elements and atmosphere control components (i.e., nozzles). Due to the low temperature of expanded nitrogen, which is supplied to maintain the oxygen level below a specified limit, its flow rate affects the cooling of the chamber temperature. The load in the furnace, depending on its mass, heat capacity, and residence time in each chamber, also absorbs heat from the chamber. Both of these phenomena are monitored by a thermostat, which strives to maintain the temperature set in the heating profile. The heating power, nitrogen flow rate, and thermostat operating range are empirically determined for the assumed load mass of a given type of AHEx based on technological trials.

A single AHEx inside the furnace chamber is characterized by a resultantly lower load heat capacity, as opposed to the expected mass of an entire production batch. In practice, this means slower cooling of the furnace chamber, leading to an anticipated increase in the temperature affecting the single AHEx unit via convection.

The omission of brazing jigs was associated with their expected role as heat sinks, which results from the heat capacity and density of stainless steel 316L. The lower heat capacity of the steel means it heats up faster. Thus, in transitions between furnace chambers, outside the zones of direct influence of the heating elements, the brazing jigs will retain and transfer heat to the AHExs through conduction.

Additionally, the absence of brazing jigs exposes a larger surface area of the AHExs to thermal radiation. Measures with the NS800 spectrophotometer showed nearly a twofold difference in the measured brightness L^* between the AHExs and the used brazing jigs (45.25 and 27.58 [cd/m²], respectively). This indirectly affects the reduction of the emissivity coefficient for the AHEx, thereby reflecting a greater amount of thermal radiation that could have been absorbed by the brazing jigs. Consequently, without brazing jigs, the heat conduction effect is bypassed, limiting the achievable maximum temperature inside the AHEx.

ACKNOWLEDGEMENTS

The research was conducted as a part of the Applied Doctorate Program of the Ministry of Education and Science implemented in the years 2021–2025 (Agreement No. DWD/(PP) RU00019673). The partner of the conducted research is MAHLE Behr Ostrów Wielkopolski Sp. z o.o.

REFERENCES

- [1] D. Brough and J. Hussam, "The aluminium industry: A review on state-of-the-art technologies, environmental impacts and possibilities for waste heat recovery," *Int. J. Thermofluids*, vol. 12, pp. 25–28, 2020, doi: [10.1016/j.ijft.2019.100007](https://doi.org/10.1016/j.ijft.2019.100007).
- [2] K. Thulukkanam, *Heat Exchanger Design Handbook*, 2nd ed. Boca Raton, FL, USA: CRC Press, 2013, doi: [10.1201/b14877](https://doi.org/10.1201/b14877).
- [3] R. Hamod, "Review on the HVAC System Modeling Types and the Shortcomings of Their Application," *J. Energy*, vol. 2013, p. 768632, 2013, doi: [10.1155/2013/768632](https://doi.org/10.1155/2013/768632).
- [4] European Aluminium Association, *The Aluminium Automotive Manual*, Applications – Power Train – Heat Exchangers, 2011, pp. 14–43.
- [5] Statista, "Estimated worldwide motor vehicle production between 2019 and 2023, by type," [Online]. Available: <https://www.statista.com/statistics/1097293/worldwide-motor-vehicle-production-by-type/>. [Accessed: Aug. 5, 2024].
- [6] R.K. Shah and D.P. Sekulic, *Fundamentals of Heat Exchanger Design*. Hoboken, NJ, USA: John Wiley & Sons, 2003, pp. 78–96.
- [7] A. Winiowski, "Brazeability – the definitions and examples of its investigation," *Weld. Rev.*, vol. 9, pp. 58–62, 2010.
- [8] Y. Wu, C. Yu, and D.P. Sekulic, "Si diffusion across the liquid/solid interface of capillary-driven (Al–Si)–K–Al_{mx}F_yz micro-layers," *J. Mater. Sci.*, vol. 56, pp. 7681–7697, 2021, doi: [10.1007/s10853-020-05689-x](https://doi.org/10.1007/s10853-020-05689-x).
- [9] H. Zhao and R. Woods, "Controlled atmosphere brazing of aluminum," in *Advances in Brazing: Science, Technology and Applications*, M.K. Krishnan, Ed., Cambridge, UK: Woodhead Publishing, 2013, pp. 280–322, doi: [10.1533/9780857096500.2.280](https://doi.org/10.1533/9780857096500.2.280).
- [10] Z. Mirski and J. Pabian, "Modern trends in production of brazed heat exchangers for automotive industry," *Weld. Rev.*, vol. 89, no. 8, pp. 18–24, 2017, doi: [10.26628/ps.v89i8.798](https://doi.org/10.26628/ps.v89i8.798).
- [11] European Aluminium Association, "EAA Aluminium Automotive Manual – Joining," in *The Aluminium Automotive Manual*, 2015, pp. 21–22.
- [12] W. Pudlik, *Wymiana i wymienniki ciepła [Heat Exchange and Heat Exchangers]*, student textbook, R. Kazimierzczak, Ed., Gdańsk, Poland: Wydawnictwo Politechniki Gdańskiej, 2012, pp. 7–14.
- [13] Z. Gao, Z. Qin, and Q. Lu, "Controlled atmosphere brazing of 3003 aluminum alloy using low-melting-point filler metal fabricated by melt-spinning technology," *Materials*, vol. 15, no. 17, p. 6080, 2022, doi: [10.3390/ma15176080](https://doi.org/10.3390/ma15176080).
- [14] L. Bitschnau and M. Kozek, "Modeling and control of an industrial continuous furnace," in *Proc. Int. Conf. Comput. Intell., Model. Simul.*, Vienna, Austria, 2009, doi: [10.1109/CSSim.2009.26](https://doi.org/10.1109/CSSim.2009.26).
- [15] Z. Mirski, J. Pabian, T. Wojdat, and J. Hejna, "Significance of the brazing gap in the brazing of aluminium heat exchangers for automotive industry," *Weld. Technol. Rev.*, vol. 92, no. 4, pp. 7–14, 2020, doi: [10.26628/wtr.v92i3.1114](https://doi.org/10.26628/wtr.v92i3.1114).
- [16] "RotoPaq Lite: Datapaq's new temperature profiling system," *Polski Przemysł*, 2014. [Online]. Available: <https://polskiprzemysl.com.pl/produkty/rotopaq-lite-nowy-system-profilowania-temperatury-firmy-datapaq/>. [Accessed: Jul. 16, 2024].
- [17] S. Nadolny, A. Hamrol, M. Rogalewicz, and A. Piasecki, "Measurement methods for flux residue quantity after controlled atmosphere brazing of aluminum coolers," *Manag. Prod. Eng. Rev.*, vol. 14, no. 3, pp. 156–163, 2023, doi: [10.24425/mper.2023.147197](https://doi.org/10.24425/mper.2023.147197).
- [18] S. Nadolny and M. Rogalewicz, "Transition of controlled atmosphere brazing jig for aluminum heat exchangers from spring-loaded to fixed-dimension," in *Adv. Manuf. IV, Proc. MANUFACTURING 2024 Conf.*, 2024, pp. 1–13, doi: [10.1007/978-3-031-56467-3](https://doi.org/10.1007/978-3-031-56467-3).

- [19] F. He, Z.-X. Wang, G. Liu, and X.-L. Wu, "Calculation model, influencing factors, and dynamic characteristics of strip temperature in a radiant tube furnace during continuous annealing process," *Metals*, vol. 12, no. 8, p. 1256, 2022, doi: [10.3390/met12081256](https://doi.org/10.3390/met12081256).
- [20] P. Tutak, "Thermal stresses in air coolers supercharged resulting from their validation process," (in Polish), Ph.D. dissertation, Poznan Univ. Technol., Poznań, Poland, 2019.
- [21] P. Heitjans and J. Kärger, *Diffusion in Condensed Matter: Methods, Materials, Models*, 2nd ed., Basel, Switzerland: Birkhäuser, 2005, pp. 3–64, doi: [10.1007/3-540-30970-5](https://doi.org/10.1007/3-540-30970-5).
- [22] J. Ågren, *The Role of Diffusion in Materials*. Stockholm, Sweden: Thermo-Calc Software AB, 2019.
- [23] C. Ho, R. Powell, and P. Liley, "Thermal conductivity of the elements," *J. Phys. Chem. Ref. Data*, Suppl. no. 1, pp. 279–421, 1974.
- [24] D. Kong *et al.*, "Mechanical properties and corrosion behavior of selective laser melted 316L stainless steel after different heat treatment processes," *J. Mater. Sci. Technol.*, vol. 35, no. 7, pp. 1499–1507, 2019, doi: [10.1016/j.jmst.2019.03.003](https://doi.org/10.1016/j.jmst.2019.03.003).
- [25] S. Eshkabilov, I. Ara, I. Sevostianov, F. Azarmi, and X. Tangpong, "Mechanical and thermal properties of stainless steel parts, manufactured by various technologies, in relation to their microstructure," *Int. J. Eng. Sci.*, vol. 159, p. 103398, 2021, doi: [10.1016/j.ijengsci.2020.103398](https://doi.org/10.1016/j.ijengsci.2020.103398).
- [26] A. Goldasz, Z. Malinowski, and A. Cebo-Rudnicka, "Thermo-mechanical analysis of the charge heating in a rotary furnace," *Arch. Metall. Mater.*, vol. 64, no. 4, pp. 1377–1384, 2019, doi: [10.24425/amm.2019.130104](https://doi.org/10.24425/amm.2019.130104).
- [27] M. Poková, M. Cieslar, and J. Lacaze, "Enhanced AW3003 aluminum alloys for heat exchangers," in *Proc. WDS'11 Contrib. Papers, Part III*, 2011, pp. 141–146.
- [28] J. Wu, *A Basic Guide to Thermocouple Measurements*, Texas Instruments, Appl. Rep. SBAA274, 2018.
- [29] M. Ainali, A. Falkeno, and R. Robinson, *Brazing Handbook*, CuproBraz, 8th ed., 2006, pp. 47–56.
- [30] A. Zhang and Y. Li, "Effect of alloying elements on thermal conductivity of aluminum," *Materials*, vol. 16, no. 8, p. 2972, 2023, doi: [10.3390/ma16082972](https://doi.org/10.3390/ma16082972).
- [31] "Aluminum Alloy 3003 (UNS A93003)," Matmake. [Online]. Available: <https://matmake.com/materials-data/aluminum-3003-properties.html>. [Accessed: Jul. 16, 2024].
- [32] J. Arblaster, *Selected Values of the Crystallographic Properties of Elements*. Materials Park, OH, USA: ASM Int., 2018.
- [33] W. Malcom and J. Chase Jr., "NIST-JANA thermochemical tables," *J. Phys. Chem. Ref. Data*, 4th ed., Part I, Al-Co, 1998.
- [34] "Heat storage in materials," The Engineering Toolbox. [Online]. Available: https://www.engineeringtoolbox.com/sensible-heat-storage-d_1217.html. [Accessed: Jul. 16, 2024].
- [35] G. Fugallo, A. Cepellotti, L. Paulatto, M. Lazzeri, N. Marzari, and F. Mauri, "Thermal conductivity of graphite and graphite: Collective excitations and mean free paths," *Nano Lett.*, vol. 14, no. 11, pp. 6109–6114, 2014, doi: [10.1021/nl502059f](https://doi.org/10.1021/nl502059f).
- [36] L. Zhao, J. Tang, M. Zhou, and K. Shen, "A review of the coefficient of thermal expansion and thermal conductivity of graphite," *New Carbon Mater.*, vol. 37, no. 3, pp. 544–555, 2022, doi: [10.1016/S1872-5805\(22\)60603-6](https://doi.org/10.1016/S1872-5805(22)60603-6).
- [37] CT Carbon GmbH, *CGT-75 Material Data Sheet*. [Online]. Available: www.cgt-carbon.pl. [Accessed: Jul. 17, 2024].
- [38] J. Ziman, *Electrons and Phonons: The Theory of Transport Phenomena in Solids*. New York, NY, USA: Oxford Univ. Press, 2001.